

# A hybrid method for determining particle masses at the Large Hadron Collider with fully identified cascade decays

---

**Mihoko M. Nojiri,**

*Theory Group, KEK and the Graduate University for Advanced Study (SOUKENDAI),  
1-1 Oho, Tsukuba, 305-0801, Japan  
and  
Institute for the Physics and Mathematics of the Universe (IPMU), University of Tokyo,  
5-1-5 Kashiwa-noHa, Kashiwa City, Chiba 277-8568, Japan  
E-mail: [nojiri@post.kek.jp](mailto:nojiri@post.kek.jp)*

**Giacomo Polesello,**

*INFN, Sezione di Pavia, Via Bassi 6, 27100 Pavia, Italy  
E-mail: [giacomo.polesello@cern.ch](mailto:giacomo.polesello@cern.ch)*

**Daniel R. Tovey,**

*Department of Physics and Astronomy,  
University of Sheffield, Hounsfield Road, Sheffield S3 7RH, UK  
E-mail: [daniel.tovey@cern.ch](mailto:daniel.tovey@cern.ch)*

**ABSTRACT:** A new technique for improving the precision of measurements of SUSY particle masses at the LHC is introduced. The technique involves kinematic fitting of events with two fully identified decay chains. We incorporate both event  $E_T^{miss}$  constraints and independent constraints provided by kinematic end-points in experiment invariant mass distributions of SUSY decay products. Incorporation of the event specific information maximises the information used in the fit and is shown to reduce the mass measurement uncertainties by  $\sim 30\%$  compared to conventional fitting of experiment end-point constraints for the SPS1a benchmark model.

**KEYWORDS:** SUSY, fit, end-point, hybrid.

---

## Contents

<b>1. Introduction</b>	<b>1</b>
<b>2. Description of technique</b>	<b>2</b>
<b>3. Example: <math>n = 4</math> step symmetric decay chain</b>	<b>3</b>
3.1 General discussion	3
3.2 Concrete example: $\tilde{q}_L$ decays at the SPS1a mSUGRA benchmark point	5
<b>4. Conclusions</b>	<b>9</b>

---

## 1. Introduction

Measurement of SUSY particle masses in R-parity conserving SUSY events at hadron colliders such as the LHC is complicated by a number of factors. First, imperfect detector hermeticity close to the beam-pipe and our ignorance of the initial state parton momentum prevent measurement of the final state momentum in the  $z$ (beam)-direction. This removes one kinematic constraint on the masses of particles generated in any given event. Second, the presence of an invisible Lightest SUSY Particle (LSP) at the end of each decay chain generates eight unknown four-momentum components in every event. As a result the kinematics of SUSY events at hadron colliders are typically highly under-constrained.

Several approaches to this general problem have been documented. Given a sufficiently long decay chain, constraints on analytical combinations of SUSY particle (‘sparticle’) masses can be obtained from the positions of end-points in distributions of invariant masses of combinations of visible SUSY-decay products (jets, leptons etc.) [1]. The system of equations may be solved with a numerical fit to obtain the individual masses, if enough constraints are provided [1, 2, 3].

An alternative class of techniques which does not rely on the end-point information is also available. These techniques vary the assumed LSP momenta in a given event subject to event kinematic constraints in order to construct variables sensitive to the masses of sparticles present in the event. One such technique involves the construction of the  $M_{T2}$  variable [4, 2, 5], which is usually defined for events where the same decay chain appears in both ‘legs’ of the event. For given assumed LSP transverse momenta the maximum value of the transverse masses of the two legs is calculated. This quantity is then minimised by varying the LSP momenta subject to the event  $E_T^{miss}$  constraints to give the value of  $M_{T2}$ . The end-point of the  $M_{T2}$  distribution depends on the test LSP mass  $M_{test}$  and has recently been shown to display a kink structure when  $M_{test}$  is equal to the true LSP mass

[6, 7, 8, 9]. This shows that  $E_T^{miss}$  constraints are important for obtaining the absolute mass scale of SUSY particles.

Another, more involved technique of this kind is the *mass relation method* [10]. In this method the masses of sparticles in the decay chain are calculated for a range of LSP momenta. When the decay chain present in the event involves a large number of SUSY states, the calculated sparticle masses are constrained to lie on a hypersurface in the mass parameter space, and the intersection of several such hypersurfaces from different events determines the true particle masses. Alternatively the existence of solutions to the system of mass-shell conditions provided by under-constrained events can be used to constrain the individual masses [11].

The techniques described above all seek to determine the masses of particles appearing in kinematically under-constrained events by combining information from multiple events, either explicitly, as in the *mass-relation method*, or implicitly by obtaining constraints from distributions of quantities derived from individual events. This paper describes a simple extension of these techniques (the *hybrid method*) in which information from multiple events is combined with event information in a kinematic fit to fully reconstruct events and hence constrain the masses of individual SUSY particles. In this paper, we especially emphasize a case where both legs contain the same cascade decay chain, so that events are more prominent over the background, and fewer unknown mass parameters are required. It is also possible to include  $E_T^{miss}$  constraints for this case, which provide independent information on the LSP mass. Full reconstruction of SUSY particle kinematics with this technique could also be useful for other purposes such as measuring the spin-statistics of SUSY states.

Section 2 introduces the new technique while Section 3 discusses a particular example of its application and illustrates the improvement in mass measurement precision obtained for a specific benchmark SUSY model. Section 4 concludes and outlines directions for future work.

## 2. Description of technique

To simplify the description, we first examine the case where a specific decay chain appears in both legs of the event. Such ‘symmetric’ events will possess a considerably smaller branching ratio than ‘single-leg’ events containing only one such decay chain but the additional decay products can lead to striking signatures which strongly suppress the SM and SUSY backgrounds. Conversely, if such events are observable then it is also probable that significant numbers of single-leg events can also be observed. Both classes of event are used by the technique described here.

Our strategy is as follows. We start with constraints on sparticle masses obtained from kinematic end-points in distributions of invariant mass combinations obtained from single-leg events, as described in Section 1. Because one of each of these distributions is obtained from the experimental data-set considered we call these constraints ‘experiment-wise’. In addition to such constraints, we possess ‘event-wise’ constraints which are obtained from mass-shell conditions provided by the event visible decay products and LSP momenta, where the latter are further constrained by the measured event  $E_T^{miss}$  components. A

kinematic fit to both the experiment-wise and event-wise constraints can possess fewer degrees-of-freedom than the simple experiment-wise end-point fit, potentially improving the sparticle mass precision.

In practice event visible momenta and  $E_T^{miss}$  values may be measured with limited precision causing each individual kinematic fit to generate mass values which potentially deviate more from the true masses than the equivalent quantities obtained from the experiment-wise end-point fit. Nevertheless because the data-set provides us with a number of uncorrelated candidate events, the means of all the fitted event mass values can indeed improve the mass measurement precision. The situation is analagous to measuring the mass of a resonance decaying to visible decay products - the mass value obtained from one event may be relatively inaccurate but the uncertainty is reduced by considering the mean mass obtained from all events.

It is instructive to consider at this point the roles played by the different constraints in the event-wise fits in this simplified case of symmetric events. Each leg of the event contributes four unknown LSP four-momentum components to the degrees-of-freedom of the event, while for a decay chain consisting of  $n$  steps each leg contributes  $n$  mass-shell conditions. Let us define the number of degrees-of-freedom of the experiment-wise end-point fit to be  $d_{end} = n_{mass} - c_{end}$ , where  $n_{mass}(= n)$  is the number of sparticle masses and  $c_{end}$  is the number of uncorrelated end-point constraints. In this case the *extra* number of degrees-of-freedom generated by including the event-wise information is  $d_{evt} = n_{mom} - c_{evt}$ , where  $n_{mom}$  is the number of unknown LSP four-momentum components and  $c_{evt}$  is the number of event-wise constraints. The condition for inclusion of the event-wise information to potentially improve the mass precision is  $d_{evt} < 0$ .

For symmetric events  $d_{evt}$  is given by  $4 - n$  for one leg and respectively  $6 - 2n$  or  $8 - 2n$  for two legs with or without  $E_T^{miss}$  constraints applied. Consequently if  $n > 4$  even considering one leg alone in conjunction with the end-point constraints potentially improves the mass measurement precisions, while if  $n > 3$  improved precisions can potentially be obtained by using both legs with  $E_T^{miss}$  constraints.

It should be noted that given an unambiguous assignment of visible final states to decay chain steps, the technique described here could be extended to non-symmetric events where some/all of the SUSY states appear in both legs of the event. In this case, for  $n_1$  and  $n_2$  steps in legs 1 and 2,  $d_{evt}$  is given by  $6 - (n_1 + n_2)$  or  $8 - (n_1 + n_2)$  when including or excluding the event-wise  $E_T^{miss}$  constraints. Consequently if  $n_1 + n_2 > 6$  improved mass measurement precisions can be obtained by using event-wise fits with  $E_T^{miss}$  constraints applied.

### 3. Example: $n = 4$ step symmetric decay chain

#### 3.1 General discussion

Let us now consider an example of mass measurement using symmetric events, for the specific case of  $n = 4$ . The decay chain present in both legs is

$$\delta \rightarrow \gamma c \rightarrow \beta bc \rightarrow \alpha abc, \quad (3.1)$$

where Greek letters denote SUSY states, Roman letters denote visible SM decay products and  $\alpha$  is the LSP. Denoting the two legs of the event with subscripts 1 and 2, the eight mass-shell conditions are:

$$\begin{aligned}
(p(a_1) + p(b_1) + p(c_1) + p(\alpha_1))^2 &= (p(a_2) + p(b_2) + p(c_2) + p(\alpha_2))^2 = m_\delta^2, \\
(p(a_1) + p(b_1) + p(\alpha_1))^2 &= (p(a_2) + p(b_2) + p(\alpha_2))^2 = m_\gamma^2, \\
(p(a_1) + p(\alpha_1))^2 &= (p(a_2) + p(\alpha_2))^2 = m_\beta^2, \\
(p(\alpha_1))^2 &= (p(\alpha_2))^2 = m_\alpha^2.
\end{aligned} \tag{3.2}$$

To these constraints should be added the two constraints provided by the event  $E_T^{miss}$  components:

$$\begin{aligned}
p_x(\alpha_1) + p_x(\alpha_2) &= E_x^{miss}, \\
p_y(\alpha_1) + p_y(\alpha_2) &= E_y^{miss},
\end{aligned} \tag{3.3}$$

thus giving ten event-wise constraints in total (i.e.  $c_{evt} = 10$ ). The number of unknown parameters appearing in these constraints is twelve – eight LSP four-momentum components together with four unknown sparticle masses. With the definitions from Section 2 the number of extra unknown parameters present in the event-wise fit relative to the end-point fit is therefore  $n_{mom} = 8$ . Consequently  $d_{evt} = -2$  indicating a potential gain over the end-point fit. In practice the four mass-shell conditions for each leg may be solved analytically to give a locally invertible map from the four sparticle masses to the four components of the LSP four momentum. In this case  $c_{evt} = 2$  and  $n_{mom} = 0$ , however  $d_{evt}$  is clearly unchanged.

It is also interesting to consider the above example when  $E_T^{miss}$  constraints are not included in the event-wise fit. In this case  $n_{mom} = 8$  and  $c_{evt} = 8$  (or equivalently  $n_{mom} = 0$  and  $c_{evt} = 0$  if solving the mass-shell conditions) and hence  $d_{evt} = 0$ . Each leg of the event is independent and the event-wise constraints just map sparticle masses to LSP four momenta. The event-wise fit is therefore equivalent to solving the kinematic end-point mass constraints and no gain in mass precision is obtained. The situation changes when the  $E_T^{miss}$  constraints are applied because in this case the kinematics of the two legs are connected.

Note that an alternative, related, approach to this  $n = 4$  problem can also be taken. Namely, one merely utilises the equivalence of the fitted masses in the two legs of the event. In this case the constraints in Eqns. 3.2 and 3.3 reduce in number to six (since the masses appearing in Eqn. 3.2 are *a priori* unconstrained) and hence two degrees-of-freedom remain ( $d_{evt} = 2$ ). Thus each event is under-constrained. The LSP four-momenta which satisfy the constraints for a given event define a two-dimensional surface in the four-dimensional  $m_\alpha, m_\beta, m_\gamma, m_\delta$  space. If a few events of this kind can be found, it is possible to solve for the masses, which are given by the coordinates of the point of intersection of all the event 2D surfaces in the 4D space. This approach is similar to the mass relation method described in the introduction and will be studied in full in a future paper.

### 3.2 Concrete example: $\tilde{q}_L$ decays at the SPS1a mSUGRA benchmark point

Let us now examine in detail a concrete realisation of the decay chain discussed above. At mSUGRA point SPS1a there is a significant branching ratio for the decay chain

$$\tilde{q}_L \rightarrow \tilde{\chi}_2^0 q \rightarrow \tilde{l}_R l q \rightarrow \tilde{\chi}_1^0 l l q. \quad (3.4)$$

This chain provides 5 kinematic end-point mass constraints from invariant mass combinations of jets and leptons [12]:

- $m(ll)^{max} = 77.08 \pm 0.08(\text{scale}) \pm 0.05(\text{stat}) \text{ GeV}$
- $m(llq)^{max} = 431.1 \pm 4.3(\text{scale}) \pm 2.4(\text{stat}) \text{ GeV}$
- $m(llq)^{min} = 203.0 \pm 2.0(\text{scale}) \pm 2.8(\text{stat}) \text{ GeV}$
- $m(lq)_{hi}^{max} = 380.3 \pm 3.8(\text{scale}) \pm 1.8(\text{stat}) \text{ GeV}$
- $m(lq)_{lo}^{max} = 302.1 \pm 3.0(\text{scale}) \pm 1.5(\text{stat}) \text{ GeV}$

For this study unbiased samples equivalent to  $100 \text{ fb}^{-1}$  (one Monte Carlo ‘experiment’) of SPS1a signal events and  $t\bar{t}$  background events were generated with HERWIG 6.4 [13, 14] and passed to a generic LHC detector simulation [15]. A lepton reconstruction efficiency of 90% was assumed.

Events were selected in which the above decay chain appears in both legs of the event with the following requirements:

- $N_{jet} \geq 2$ , with  $p_T(j2) > 100 \text{ GeV}$ ,
- $M_{eff2} = E_T^{miss} + p_T(j1) + p_T(j2) > 100 \text{ GeV}$ ,
- $E_T^{miss} > \max(100 \text{ GeV}, 0.2M_{eff2})$ ,
- $N_{lep} = 4$ , where  $lep = e/\mu(\text{isolated})$  and  $p_T(l4) > 6 \text{ GeV}$ ,
- 2 Opposite Sign Same Flavour (OSSF) lepton pairs. If the pairs are of different flavour both pairs must have  $m(ll) < m(ll)^{max}$ . If both pairs are of the same flavour then one and only one of the two possible pairings must give two  $m(ll)$  values which are both less than  $m(ll)^{max}$ . These pairings allocate the leptons to each leg of the event.
- One and only one possible pairing of the two leading jets with the two OSSF lepton pairs must give two  $m(llq)$  values less than  $m(llq)^{max}$ . These pairings allocate the jets to each leg of the event.
- For each inferred leg of the event the maximum(minimum) of the two  $m(lq)$  values must be less than  $m(lq)_{hi(lo)}^{max}$ . This ordering allocates the leptons to the *near* and *far* [2] positions in the decay chain.

The requirement of 4-leptons in two OSSF pairs and two high- $p_T$  jets consistent with kinematic end-points, together with large  $E_T^{miss}$ , is effective at removing the majority of SM and SUSY backgrounds (see below).

Each selected event was fitted with MINUIT [16]. Free parameters were taken to be the four masses appearing in the decay chain:  $m(\tilde{q}_L)$ ,  $m(\tilde{\chi}_2^0)$ ,  $m(\tilde{l}_R)$  and  $m(\tilde{\chi}_1^0)$ . In the spirit of the discussion in Section 3.1 the mass-shell conditions and measured momenta of the visible decay products for each leg were solved to determine the LSP four-momenta, giving two solutions for each leg. The  $\chi^2$  minimisation function was defined by:

$$\begin{aligned} \chi^2 = & \left( \frac{m(ll)_{evt}^{max} - m(ll)_{expt}^{max}}{\sigma_{m(ll)^{max}}} \right)^2 \\ & + \left( \frac{m(llq)_{evt}^{max} - m(llq)_{expt}^{max}}{\sigma_{m(llq)^{max}}} \right)^2 + \left( \frac{m(llq)_{evt}^{min} - m(llq)_{expt}^{min}}{\sigma_{m(llq)^{min}}} \right)^2 \\ & + \left( \frac{m(lq)_{hi;evt}^{max} - m(lq)_{hi;expt}^{max}}{\sigma_{m(lq)_{hi}^{max}}} \right)^2 + \left( \frac{m(lq)_{lo;evt}^{max} - m(lq)_{lo;expt}^{max}}{\sigma_{m(lq)_{lo}^{max}}} \right)^2 \\ & + \left( \frac{p_x(\tilde{\chi}_1^0(1)) + p_x(\tilde{\chi}_1^0(2)) - E_x^{miss}}{\sigma_{E_x^{miss}}} \right)^2 + \left( \frac{p_y(\tilde{\chi}_1^0(1)) + p_y(\tilde{\chi}_1^0(2)) - E_y^{miss}}{\sigma_{E_y^{miss}}} \right)^2, \end{aligned} \quad (3.5)$$

where *evt* denotes an expected end-point value derived from the masses in the event-wise fit with the formulae of Ref. [2], and *expt* denotes a ‘measured’ experiment-wise end-point value. The uncertainties  $\sigma$  in these ‘measured’ endpoints were those quoted above. The uncertainties on the measurements of the  $x$  and  $y$  components of  $E_T^{miss}$ ,  $\sigma_{E_x^{miss}}$  and  $\sigma_{E_y^{miss}}$ , were given by  $0.5\sqrt{E_T^{sum}}$  where  $E_T^{sum}$  is the scalar sum of jet  $p_T$  of the event. This function incorporating both event-wise  $E_T^{miss}$  constraints and experiment-wise end-point constraints was evaluated for each of the four pairs of  $\tilde{\chi}_1^0$  momentum solutions obtained from solving the leg mass-shell conditions. Fitted masses were obtained when  $\chi^2$  was minimised for the event. Fitted masses were used in the subsequent analysis only if MINUIT judged the fit to have converged and  $\chi_{min}^2 < 35.0$ .

Following application of the selection cuts described above and the requirements of fit convergence and low fit  $\chi_{min}^2$  38 SUSY ‘signal’ events with the above decay chain appearing in both legs were observed. 4 SUSY background events were observed, consisting of the above decay chain in both legs but with one or two leptonically decaying staus produced in the decays of the  $\tilde{\chi}_2^0$ s. No  $t\bar{t}$  background events were observed in 100 fb $^{-1}$  equivalent data. More SM background events may be expected in a real experiment, given that effects such as charge and lepton mis-identification are not included in the fast detector simulation. The use of full **GEANT** detector simulation is required to model correctly these effects, which is beyond the scope of this paper, however given the hard kinematic selection cuts it is reasonable to assume that they are at least smaller than the negligible  $t\bar{t}$  background considered above.

Each event-wise fit generated one set of values for the sparticle masses, namely those values which minimise the broad  $\chi^2$  function in Eqn. 3.5. The distributions of these values for one Monte Carlo experiment are shown in Fig. 1. The widths of the distributions are

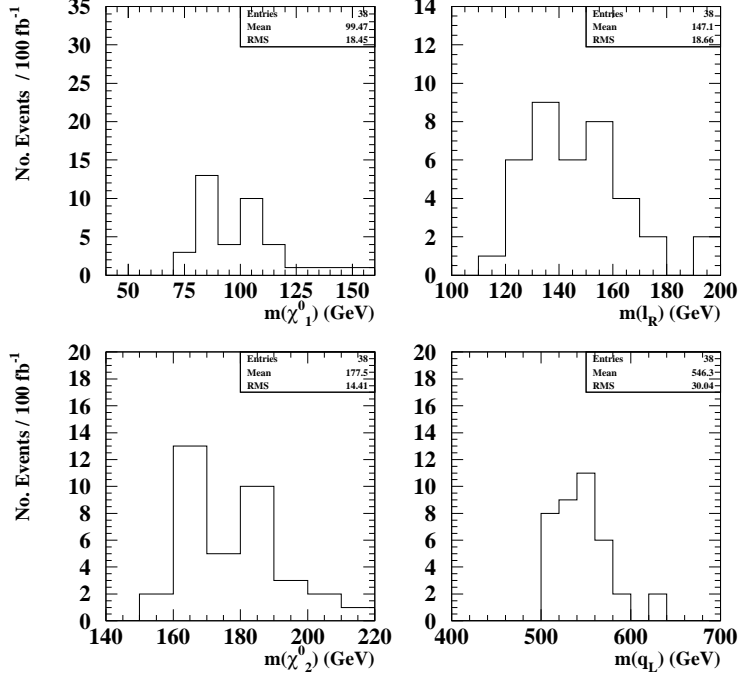


**Figure 1:** Distributions of sparticle masses obtained from event-wise fits, for one MC experiment. Each entry is obtained by minimising the  $\chi^2$  function shown in Eqn. 3.5.

greater than those which would be obtained were the  $E_T^{miss}$  constraints excluded from the fits – in that case each event-wise fit becomes equivalent to the experiment-wise end-point fit as explained in Section 3.1 and each distribution becomes a delta-function located at the equivalent mass value. The key point is that despite the fact that the mass distributions in Fig. 1 are broader when  $E_T^{miss}$  constraints are used, the means of the distributions measure the sparticle masses more accurately. This may seem counter-intuitive, however the reason is clear. The  $E_T^{miss}$  components for each event are measured with only limited precision, causing a potential shift in the minimum of the event  $\chi^2$  function away from the true sparticle masses. There is no way to correct for this effect on an event-wise basis. By correctly parameterising the  $E_T^{miss}$  measurement precision in Eqn. 3.5 however we ensure that such shifts are on average unbiased when considering all events in the experiment and hence the means of the mass distributions compensate for this resolution effect, while also making use of the reduction in degrees-of-freedom provided by the  $E_T^{miss}$  constraints. This compensation for resolution effects at the level of the experiment rather than individual events is also implicit in the end-point method where gaussian-smeared end-point functions are used when fitting the end-points in order to compensate for experimental jet and lepton energy resolutions.

In order to demonstrate the performance of the technique and judge the uncertainties in the measurements the above procedure was repeated for 100 Monte Carlo experiments.



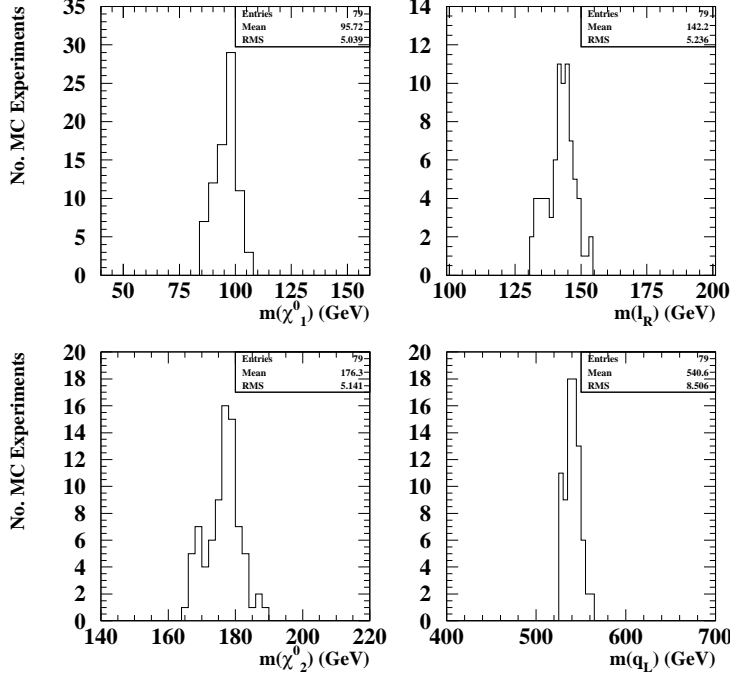


**Figure 2:** Likelihood distributions of particle masses obtained from 100 MC experiments. Each entry is the mean of an experiment-wise mass histogram such as those in Fig. 1.

For each experiment, kinematic end-point positions were sampled from gaussians with means and sigmas given by the means and uncertainties listed above. The five sampled end-point positions for each experiment were solved simultaneously with a MINUIT fit to give initial mass values for input to the MINUIT event-wise kinematic fits. For each experiment relative jet(lepton) energy scale values were sampled from gaussians of width 1%(0.1%) reflecting likely ultimate energy scale uncertainties at the LHC. Each experiment generated a set of particle mass histograms similar to those shown in Fig. 1. The means of these histograms for the 100 MC experiments were then used to construct likelihood histograms for the masses, shown in Fig. 2. The standard deviations of these histograms were taken to provide the uncertainties on the particle mass measurements.

Unbiased MC data equivalent to only one  $100 \text{ fb}^{-1}$  experiment were available for this study. For this reason the same events were used for each MC experiment, with just the end-point values and jet/lepton energy scales varying. The additional uncertainties in the final mass values expected from varying event samples were estimated from the mean statistical uncertainties in the mean experiment mass values as extracted from the event-wise distributions such as those shown in Fig. 1. We evaluated the experiment-by-experiment spread due to varying event samples as  $\sigma/\sqrt{n}$ , where  $\sigma$  is the RMS of the event-wise distributions as shown in Fig. 1, and  $n$  is the number of entries in each plot. These additional contributions were added in quadrature to the uncertainties obtained

State	Input	End-Point Fit		Hybrid Method, $E_T^{miss}$		Hybrid Method, no $E_T^{miss}$	
		Mean	Error	Mean	Error	Mean	Error
$\tilde{\chi}_1^0$	96.05	96.5	8.0	95.8(92.2)	5.3(5.5)	97.7(96.9)	7.6(8.0)
$\tilde{l}_R$	142.97	143.3	7.9	142.2(138.7)	5.4(5.6)	144.5(143.8)	7.8(8.1)
$\tilde{\chi}_2^0$	176.81	177.2	7.7	176.4(172.8)	5.3(5.4)	178.4(177.6)	7.6(7.9)
$\tilde{q}_L$	537.2–543.0	540.4	12.6	540.7(534.8)	8.5(8.7)	542.9(541.4)	12.2(12.7)

**Table 1:** Summary of mass measurement precisions for SPS1a states. Column 2 lists masses used in the **HERWIG** generator, Columns 3 and 4 the fitted masses and uncertainties obtained from the conventional fit to kinematic end-points, Columns 5 and 6 the equivalent values obtained with the new technique and Columns 7 and 8 the equivalent values obtained with the new technique excluding  $E_T^{miss}$  constraints. Figures in parentheses are those obtained with the biased sample of non-repeated events. All masses are in GeV. The quoted mass range for  $\tilde{q}_L$  excludes  $\tilde{b}$  squarks, which are produced less readily than the light squarks.

from the study. This approximation was checked with a second sample of SPS1a events equivalent to 100 different MC experiments, biased to force gluinos to decay to  $\tilde{q}_L$ ,  $\tilde{b}$  or  $\tilde{t}$ ,  $\tilde{q}_L$  to decay to  $\tilde{\chi}_2^0$  and  $\tilde{\chi}_2^0$  to decay to  $\tilde{e}$  or  $\tilde{\mu}$ . Excluding the SUSY background from this sample was estimated to bias the mean mass values by  $< 1\%$  and increase the uncertainties by  $\lesssim 5\%$ . The uncertainties increase when the SUSY background is excluded because the effect of the decrease in event statistics outweighs the reduction in bias caused by excluding the primarily  $\tilde{\tau}$  background events, which have similar kinematics to the  $\tilde{e}$  and  $\tilde{\mu}$  signal events.

The results of this study are summarised in Table 1. For comparison purposes the analysis was initially carried out with the  $E_T^{miss}$  constraints removed from the  $\chi^2$  function. The measurement precisions are consistent with those obtained from the conventional end-point fitting method, as expected following the reasoning outlined in Section 3.1. The analysis was then repeated including the  $E_T^{miss}$  constraints, giving an overall improvement in sparticle mass precisions  $\sim 30\%$  for all four masses considered. A similar improvement was found when using the biased sample of non-repeated events for different experiments. The measurement of mass differences is also improved, with for instance  $m(\tilde{q}_L) - m(\tilde{\chi}_1^0)$  being measured with a precision of 4 GeV comparable with the natural widths of the light squarks ( $\sim 5$  GeV at SPS1a) and their mass differences ( $\sim 6$  GeV). Further improvement in mass measurement precision therefore probably requires that such effects be taken into account, for instance in the definition of the  $\chi^2$  function in Eqn. 3.5.

## 4. Conclusions

A new technique for improving the precision of LHC mass measurements has been outlined in which experiment-wise information, for instance invariant mass end-point constraints, are combined with event-wise kinematic information such as  $E_T^{miss}$  constraints and measured four-momenta of visible decay products. For the SPS1a model considered here the mass measurement precision was shown to improve by  $\sim 30\%$  for  $100 \text{ fb}^{-1}$  of data. SUSY models with larger branching ratios for symmetric events containing the necessary decay chain, or with more indistinct or poorly-measured kinematic end-points, might be expected

to benefit still further from application of the technique. The technique could be extended to non-symmetric events where some/all of the SUSY states appear in both legs of the event – this strategy for measuring further SUSY masses will be examined in more detail in a future paper. Full reconstruction of SUSY particle kinematics with this technique could also potentially be useful for other purposes such as measuring the spin-statistics of SUSY states.

## Acknowledgements

The authors wish to thank the organisers of the Les Houches 2007 *Physics at TeV-Scale Colliders* workshop, where the work described in this paper was first conceived. DRT wishes to acknowledge STFC for support.

## References

- [1] I. Hinchliffe, F. E. Paige, M. D. Shapiro, J. Soderqvist and W. Yao, Phys. Rev. D **55** (1997) 5520 [arXiv:hep-ph/9610544].
- [2] B. C. Allanach, C. G. Lester, M. A. Parker and B. R. Webber, JHEP **0009** (2000) 004 [arXiv:hep-ph/0007009].
- [3] D. J. Miller, P. Osland and A. R. Raklev, JHEP **0603** (2006) 034 [arXiv:hep-ph/0510356].
- [4] C. G. Lester and D. J. Summers, Phys. Lett. B **463** (1999) 99 [arXiv:hep-ph/9906349].
- [5] A. Barr, C. Lester and P. Stephens, J. Phys. G **29** (2003) 2343 [arXiv:hep-ph/0304226].
- [6] W. S. Cho, K. Choi, Y. G. Kim and C. B. Park, arXiv:0709.0288 [hep-ph].
- [7] B. Gripaios, JHEP **0802** (2008) 053 [arXiv:0709.2740 [hep-ph]].
- [8] A. J. Barr, B. Gripaios and C. G. Lester, arXiv:0711.4008 [hep-ph].
- [9] W. S. Cho, K. Choi, Y. G. Kim and C. B. Park, arXiv:0711.4526 [hep-ph].
- [10] K. Kawagoe, M. M. Nojiri and G. Polesello, Phys. Rev. D **71** (2005) 035008 [arXiv:hep-ph/0410160].
- [11] H. C. Cheng, J. F. Gunion, Z. Han, G. Marandella and B. McElrath, arXiv:0707.0030 [hep-ph].
- [12] B.K. Gjelsten, J. Hisano, K. Kawagoe, E. Lykken, D. Miller, M. M. Nojiri, P. Osland and G. Polesello in G. Weiglein *et al.* [LHC/LC Study Group], Phys. Rept. **426** (2006) 47 [arXiv:hep-ph/0410364].
- [13] G. Corcella *et al.*, JHEP **0101** (2001) 010 [arXiv:hep-ph/0011363].
- [14] S. Moretti, K. Odagiri, P. Richardson, M. H. Seymour and B. R. Webber, JHEP **0204** (2002) 028 [arXiv:hep-ph/0204123].
- [15] E. Richter-Was, arXiv:hep-ph/0207355.
- [16] F. James and M. Roos, Comput. Phys. Commun. **10** (1975) 343.